Bulletin of the Seismological Society of America, Vol. 83, No. 6, pp. 1778–1798, December 1993

EARTHQUAKE SOURCE SPECTRA IN EASTERN NORTH AMERICA

Gail M. Atkinson

Abstract

Source spectra for earthquakes of $3 \leq M \leq 7$ in eastern North America (ENA) are determined from regional seismograph recordings, strong-motion records, teleseismic data, and Modified Mercalli Intensity data. The inclusion of MMI data is made possible by the finding that the felt area of an earthquake is an accurate measure of its high-frequency spectral level at the source.

Current ground motion relations for ENA are based on a Brune source model with a stress parameter of 100 bars. This model is a poor fit to ENA source spectra for events of $M > 4$. At high frequencies (5 to 10 Hz), observed spectral amplitudes are more nearly matched by a Brune stress parameter of 200 bars; intermediate-frequency amplitudes (near 1 Hz) are matched by a stress parameter of approximately 50 bars. An empirical two-corner source model is proposed to describe ENA source spectra for events of $4 \leq M \leq 7$.

Introduction

Current methods of predicting ground motions for future earthquakes in eastern North America (ENA) are based on an assumed seismological model of source and propagation processes (Hanks and McGuire, 1981; Boore and Atkinson, 1987; Toro and McGuire, 1987). The model treats high-frequency ground motions as filtered Gaussian noise, whose underlying spectrum is determined by attenuating an average source spectrum for a given seismic moment. The validity of the technique has been established using data from western North America (Hanks and McGuire, 1981; Boore, 1983). However its reliability in application to ENA has been limited by a lack of information concerning source spectra of eastern earthquakes.

The source model generally adopted for both the east and west has been the simple Brune (1970) model, which relates the spectrum of the shear radiation to the stress released across the fault surface. The Brune model assumes a circular rupture; its radius determines the corner frequency. The high-frequency level of the source spectrum is controlled by the stress parameter (Brune, 1970; Boatwright, 1984), whereas the low-frequency level is, by definition, proportional to the seismic moment. Thus the model provides a simple interpretation of observed spectra in terms of moment magnitude and stress drop. The expression for the basic Brune acceleration spectrum near the source (horizontal component) is (Boore, 1983):

$$A(f) = CM_0(2\pi f)^2/\left[1 + (f/f_0)^2\right] \tag{1}$$

with $C = \mathscr{R}_p FV/(4\pi\rho\beta^3 R)$, and $f_0 = 4.9 \times 10^6 \beta(\Delta\sigma/M_0)^{0.3333}$ where $\mathscr{R}_p$ = average radiation pattern (0.55), F = free surface amplification (2.0), V = partition onto two horizontal components (0.71), ρ = crustal density (2.8 gm/cm^3), β = shear wave velocity (3.8 km/sec), M_0 = seismic moment (dyne-cm), R is distance and $\Delta\sigma$ = stress parameter (bars). The adopted values for the crustal constants ρ and β are applicable for the average focal depth (about 10 km) of the study events (Mereu *et al.*, 1986).

In western North America (WNA), ground motions are well predicted on average by the Brune model with a constant stress parameter of 100 bars (Hanks and McGuire, 1981; Boore, 1983), or, equivalently, a value of 70 bars, allowing for ground-motion amplifications (beyond those of the free surface) of about a factor of 2 by the near-surface sedimentary layer, coupled with the appropriate attenuation of high frequencies (Boore *et al.*, 1992). Limited studies have suggested a similar value for ENA source spectra, with the average ENA stress parameter being perhaps a factor of 2 larger than that for WNA (Kanamori and Anderson, 1975; Atkinson, 1984, 1989; Boore and Atkinson, 1987; Somerville *et al.*, 1987).

Surprisingly, the source spectrum for the Saguenay, Quebec, earthquake of 1988 differed dramatically from the Brune model. This event, with a moment magnitude (**M**) of 5.8, and *Lg* magnitude (M_N) of 6.5, was the largest event to have occurred in ENA in over 50 years and so has assumed particular importance in the interpretation of ENA ground motion predictions. The Saguenay source spectrum requires two corner frequencies: its high-frequency level is equivalent to a Brune stress parameter of approximately 500 bars, but the level at intermediate to low frequencies (less than 1 Hz) is matched by a stress parameter of less than 100 bars (Boore and Atkinson, 1992). Boatwright and Choy (1992) have shown that two corner frequencies are required to match the source spectra derived from teleseismic data for most large intraplate earthquakes (including Saguenay).

Departures from the Brune shape are expected based on models considering a rectangular (as opposed to circular) fault (Haskell, 1969; Savage, 1972; Haddon, 1992). They are also expected based on rupture models that account for fault "roughness". Examples of inhomogeneous faulting models that imply more than one corner include the Brune (1970) partial stress drop model, the asperity model (Hartzell and Brune, 1979; McGarr, 1981), the specific barrier model (Papageorgiou and Aki, 1983), and multiple-event models (Joyner and Boore, 1986; Boatwright, 1988), among others. Although the specifics vary from one model to another, the lowest corner frequency in the spectrum is generally related to the overall rupture duration (or fault length) whereas the higher corner may reflect some local-scale characteristic (e.g. asperities, barriers, etc.) of the fault surface. Not until the Saguenay earthquake has it been fully appreciated that such deviations from the simple Brune model may have significant implications for ground motions in ENA.

The purpose of this study is to establish an empirical model to describe the source spectra of ENA earthquakes as a function of seismic moment. The primary data are source spectra determined by regressions of 1500 digital seismograph recordings from the Eastern Canada Telemetered Network (ECTN). These data are supplemented by source-spectral estimates obtained for moderate-to-large historic ENA events using regional seismigraphic data (Street and Turcotte, 1977) and teleseismic data (Boatwright and Choy, 1992), and by correlations between Modified Mercalli Intensity (MMI) data and high-frequency spectral levels. These data allow definition of the 1-Hz spectral amplitude and the high-frequency spectral level (i.e., the constant amplitude level for frequencies above the highest corner frequency but below any high-frequency cut-off) for earthquakes of $4 \leq \mathbf{M} \leq 7$.

SOURCE SPECTRAL AMPLITUDES

ECTN Data ($2.5 < \mathbf{M} < 6$)

Atkinson and Mereu (1992) performed a regression analysis of approximately 100 earthquakes of Nuttli magnitude (M_N) 3 to 6.5, recorded on the 30 stations of the ECTN. The form of this regression is:

$$\log A_{ij}(f) = \log A_{i0}(f) - b \log R_{ij} - c(f)R_{ij} + \log S_j(f) \tag{2}$$

where $A_{ij}(f)$ is the observed spectral amplitude of earthquake i at station j, for frequency f, $A_{i0}(f)$ is the source amplitude of earthquake i (averaged over all azimuths), R is hypocentral distance, b is the geometric spreading coefficient, $c(f)$ is the coefficient of anelastic attenuation, and $S_j(f)$ is the site response of station j. Complexity in shape of the attenuation curve due to wave propagation effects (Burger *et al.*, 1987) was accommodated by allowing the coefficient b to take on different values in different distance ranges. The 100 source spectra, given by the terms $A_{i0}(f)$, for $1 \leq f \leq 10$ Hz, provide the primary data set for this study.

The source terms are well constrained by the data; amplitudes at $R = 10$ km can be determined to within about 0.1 log units. (Note: amplitudes quoted at a reference distance of 1 km are obtained by assuming R^{-1} attenuation from $R = 1$ km to $R = 10$ km.) The source terms agree well with results determined independently by Boatwright (this issue), using the same data set but a different inversion method. They also agree with source spectra determined from near-source strong motion data (for events which both strong-motion and regional ECTN data are available: see Boatwright, this issue). Furthermore, it has been demonstrated that the source spectra can be used, in conjunction with either the stochastic or ray-theory models, to accurately reproduce observed ground motion parameters (Atkinson and Somerville, 1993). This provides confidence in the reliability of the source spectra.

The limited bandwidth of the ECTN data ($1 \leq f \leq 10$ Hz) places constraints on the source parameters that can be determined. For events of $\mathbf{M} > 4.5$, the corner frequency is too low to allow determination of the long-period displacement level. Therefore seismic moments for all events of $\mathbf{M} > 4.5$ are based on other data sources (Boore and Atkinson, 1987; 1992). The one exception is the Mont Laurier earthquake of 1990, for which I estimate $\mathbf{M} = 4.7$ based on examination of P- and S-wave spectra.

For very small events the high-frequency spectral levels cannot be reliably determined from the ECTN data. As shown in Figure 1, the corner frequency for events of $\mathbf{M} < 3.5$ approaches 10 Hz. For these events the 10-Hz amplitude is a lower bound for the high-frequency level. Consequently the Brune stress parameter will be systematically underestimated. This leads to an apparent dependence of stress parameter on seismic moment for events of $\mathbf{M} < 4$ (Fig. 1), which limits the usefulness of the results for small magnitudes. For events of $\mathbf{M} > 4$, we would infer that the average Brune stress is somewhat greater than 100 bars, independent of seismic moment. Two events (Saguenay and Mont Laurier) have much larger stress parameters, of the order of 500 bars.

Typical source spectra for some of the earthquakes are plotted as a function of frequency in Figure 2, in comparison to the corresponding Brune model spectra for the event's seismic moment and high-frequency level. The figure also com-

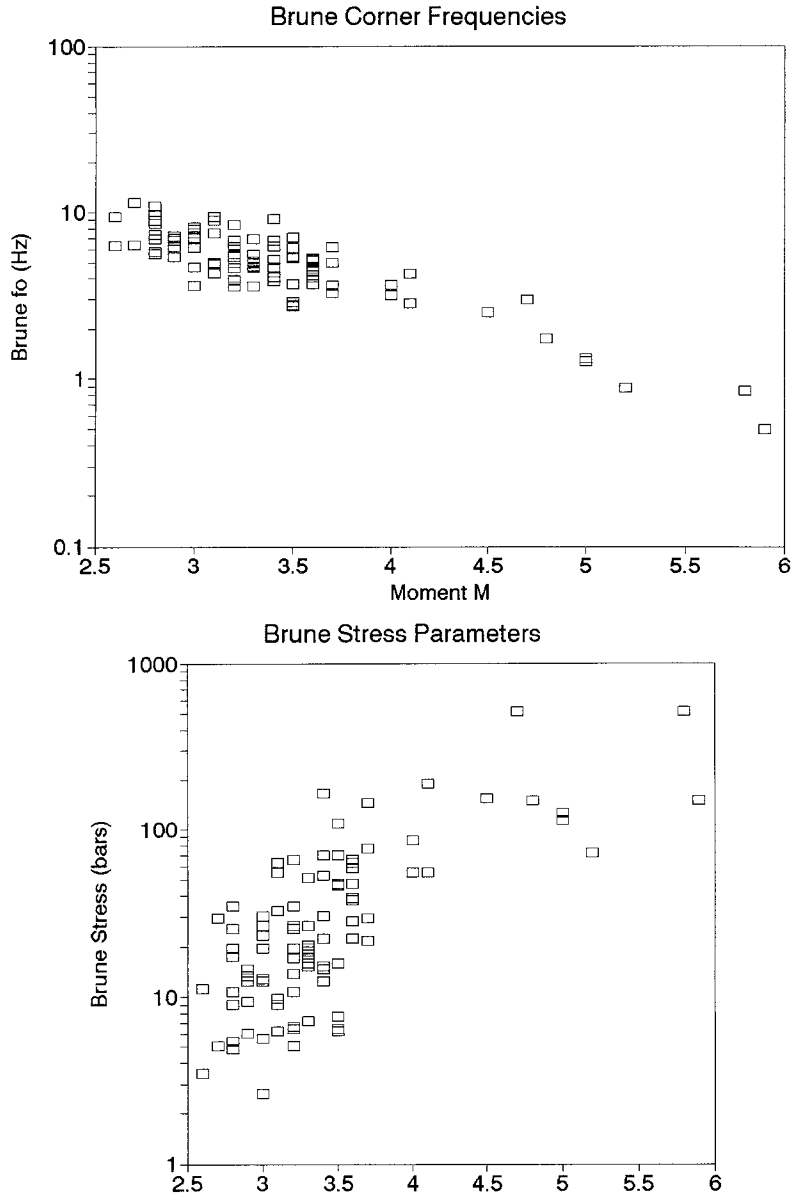

FIG. 1. Brune corner frequencies (*top* frame) and stress parameters (*bottom* frame) for the ECTN data, as a function of **M**.

pares the Atkinson-Mereu inversions to Boatwright's inversions. Small events (**M** < 4.5) are well matched by the Brune shape. For events larger than **M** 4.5, by contrast, there seems to be a deficit of intermediate-frequency energy relative to that which would be implied by the Brune model, for the given moment and high-frequency level. (Note that, for **M** > 4.5, my comparisons of the Brune model to the source spectra are based on the moments obtained from other sources, whereas the Boatwright comparisons are based on best-fit moments for the ECTN data.)

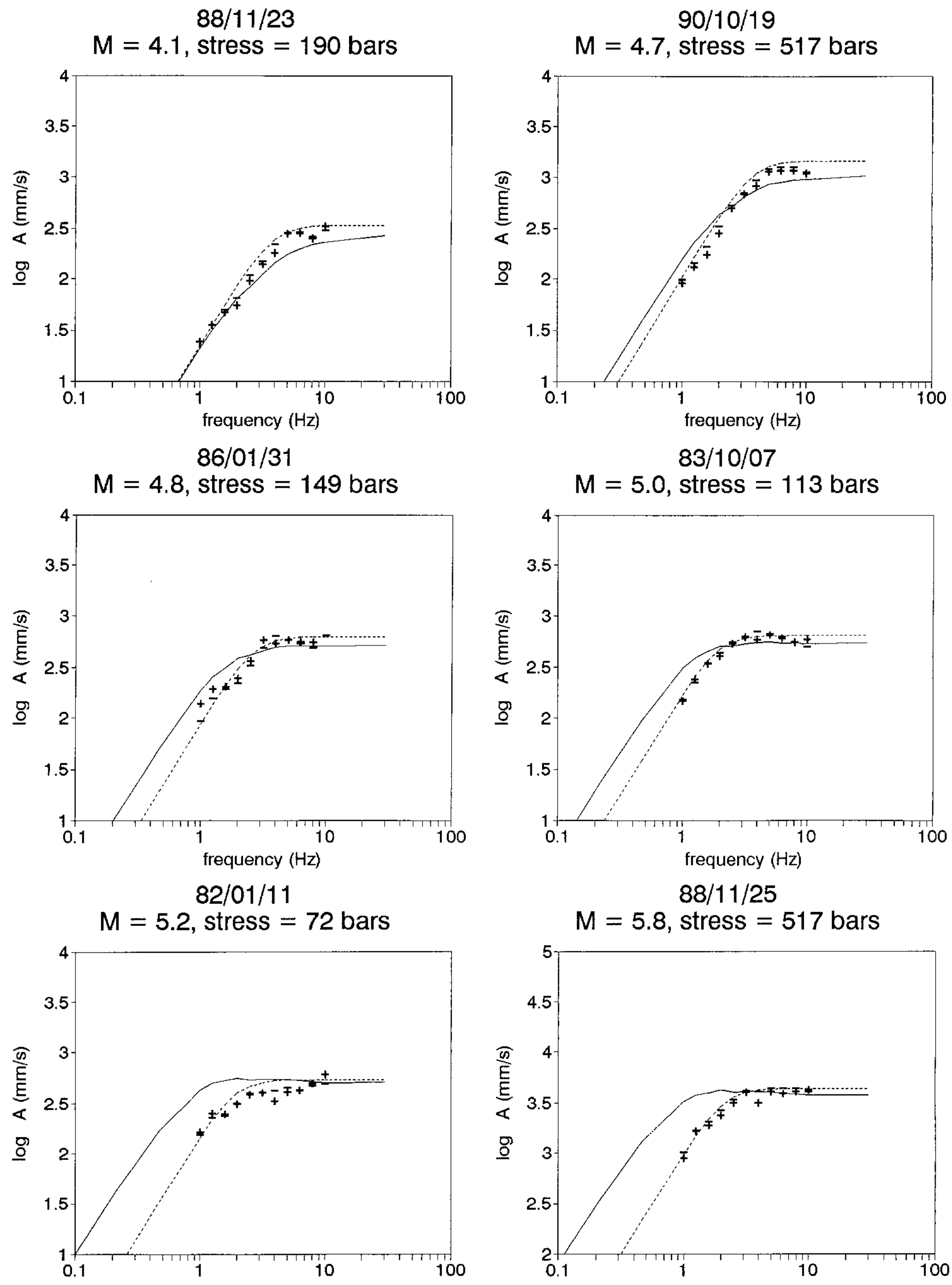

FIG. 2. Typical ECTN source spectra from Atkinson-Mereu inversion (crosses) compared with corresponding Brune spectra for the seismic moment and high-frequency level (solid lines). Inversion results of Boatwright are also shown (horizontal bars for data and dotted lines for corresponding Brune model). For events of **M** < 4.5, the seismic moment was determined from the long-period level of the spectrum. For **M** > 4.5 the moment used in my comparisons with the Brune model was obtained from other sources.

The ECTN data include only a dozen events for the magnitude range $4 \leq \mathbf{M} \leq 7$, which is of most engineering interest. Spectral parameters for these events are given in Table 1. I next describe other data for earthquakes of $4 \leq \mathbf{M} \leq 7$, from which we can estimate two spectral parameters: the 1-Hz spectral amplitude and the high-frequency level of the spectrum. Definition of these parameters as a function of seismic moment will provide the basis for an empirical spectral model covering the entire frequency band.

Other Instrumental Data on Source Spectral Amplitudes ($4 \leq \mathbf{M} \leq 7$)

There are three additional instrumental data sources from which we may estimate ENA source spectral amplitudes (see Table 1):

1. Street and Turcotte (1977) digitized regional seismographic recordings from historic earthquakes in ENA and tabulated 1-Hz source spectral amplitudes.

TABLE 1
SOURCE SPECTRAL PARAMETERS FOR $\mathbf{M} \geq 4$ EVENTS

Event	M_N	$\mathbf{M}$	A_{HF}	Stress	$A_{1\text{ Hz}}$	Data Source
250301	7.0	6.4	3.60	177	3.32	S&T, MMI
290812	5.4	4.9	2.76	130	1.97	S&T, MMI
291118		6.7	3.88	278	3.60	S&T, MMI
351101	6.3	5.8	3.52	379	3.85	S&T, MMI
391019		5.3	2.96	130	2.65	S&T, MMI
401220	5.7	5.5	2.99	102	2.35	S&T, MMI
430114		4.2			1.26	S&T
440905	5.9	5.7	3.10	106	2.45	S&T, MMI
491005		4.4			1.45	S&T
521014		4.2			1.45	S&T
570426		4.6			1.65	S&T
681109		5.4	3.38	483		MMI
751006		4.3			1.21	S&T
800827		5.1	3.00	230		MMI
820109*		4.6	2.32	48	2.02	ECTN
820109	5.7	5.5	2.91	77	2.80	B&C, MMI
820111*	5.4	5.2	2.74	72	2.20	ECTN
820119	4.5	4.0	2.19	86	1.60	ECTN
831007	5.6	5.0	2.77	113	1.60	ECTN
851005		6.7	3.55	89	3.40	B&A
851223		6.8	3.45	53	3.40	B&A
851225*		5.2	2.55	38	2.45	B&A
860131	5.0	4.8	2.75	149	1.60	ECTN
860712	4.5	4.5	2.61	154	1.60	ECTN
870610		5.0	2.88	177		MMI
880325		6.3	3.25	63	3.10	B&A
881123	4.6	4.1	2.47	190	1.60	ECTN
881125	6.5	5.8	3.61	517	1.60	ECTN
890316	5.7	5.0	2.80	126	2.60	ECTN
891225	6.1	5.9	3.30	149	3.00	ECTN
901019	5.1	4.7	3.06	517	1.60	ECTN

NOTES: Spectral levels are in log units, for mm/s, vertical component at R = 1 km. Stress is the required Brune stress, in bars, to match the observed high-frequency level. ECTN = this study; S&T = Street and Turcotte, 1977; MMI = estimated from felt area; B&C = Boatwright and Choy, 1989; B&A = Boore and Atkinson, 1989. Listed data sources are for spectral amplitudes; references for moment magnitudes are described in text.

*indicates event was an aftershock.

The attenuation correction they employed at 1 Hz agrees well with that determined by Atkinson and Mereu (1992), so their 1-Hz source spectral estimates should be consistent with those of this study.

2. Boatwright and Choy (1992) used teleseismic data ($f < 2$ Hz) to obtain source spectra for several ENA events. Their 1-Hz spectral estimates agree with estimates from ECTN or strong-motion data, for the Saguenay, Ungava, and Nahanni earthquakes. By contrast, the ECTN and strong-motion data imply larger amplitudes for the high-frequency spectral level than do the teleseismic data. I suspect this discrepancy is due to the bandwidth of the teleseismic data (too low to observe the full high-frequency level), combined with increasing uncertainty in teleseismic attenuation corrections for frequencies in the 1 to 2 Hz range. I therefore use only the 1-Hz spectral amplitudes from the Boatwright and Choy study.
3. I consider the Nahanni earthquakes to be more nearly representative of midplate than western earthquakes (Wetmiller *et al.*, 1988), and so include them in the dataset. The source spectrum for the largest event (**M** 6.8) was determined by near-source accelerograph data (Choy and Boatwright, 1988). The spectra of the smaller events were obtained from the spectral ratio of each event to that of the largest shock (Boore and Atkinson, 1989). The spectral ratios were based on regional seismographic data.

These seismographic data provide good additional information regarding 1-Hz spectral amplitudes but little information on high-frequency amplitudes, due to the bandwidth limitations of most of the instruments. Hanks and Johnston (1992) have suggested that the MMI data from historic earthquakes may contain such information.

MMI Data on Source Spectral Amplitudes ($4 \leq \mathbf{M} \leq 7$)

Table 2 lists the areas enclosed by various MMI levels, for all felt events in ENA for which we have seismographic estimates of the source spectrum. The MMI data are taken from the paper of Hanks and Johnston (1992), and from interpretation of intensity maps provided by the Geological Survey of Canada (J. Drysdale, personal comm., 1992).

The correlation between felt areas (area experiencing MMI II or greater) and high-frequency source spectral level is excellent. As shown in Figure 3 (*top* frame), the felt area of an earthquake allows us to estimate its high-frequency source-spectral level with surprising precision:

$$\log A_{HF} = -2.73 + 0.99 \log a_f \tag{3}$$

where A_{HF} is the vertical component at a distance of $R = 1$ km, in millimeters per second and a_f is the felt area in square kilometers. The standard deviation of log A_{HF} residuals (σ) is only 0.12. This may be partly fortuitous because the uncertainties in estimating felt areas, although unknown, are probably of this order; nevertheless it indicates that felt area is a remarkably good predictor of high-frequency source spectral level.

Interestingly, the felt area seems to be a slightly more precise measure of the high-frequency source spectrum than is the area of stronger shaking (compare symbols for MMI V and felt areas of Fig. 3). Felt area is probably less variable than the area of stronger shaking because soil effects are averaged over a larger region; felt area is also less sensitive to the location of population centers

TABLE 2

MMI AREAS FOR EVENTS WITH SEISMOGRAPHIC SOURCE SPECTRAL DATA
SOURCE SPECTRAL AMPLITUDES IN MM / S, VERT. COMPONENT, R = 1 KM

	MMI areas (km**2)						
Date	log a_f	log a_{IV}	log a_V	log a_{VI}	**M**	log A_{HF}	log A_1
250301	6.41	5.83	5.14	4.80	6.4		3.32
290812	5.56		4.45	3.40	4.9		1.92
291118	6.70	6.32	5.95	5.43	6.7		3.55
351101	6.33	5.89	5.11	4.60	5.8		3.80
401220	5.79	5.34	4.67	3.42	5.5		2.30
440905	5.91	5.57	5.07	4.36	5.7		2.40
820109	5.14	4.05	3.70		4.6	2.32	2.02
820109	5.71	5.36	4.89	3.38	5.5		2.80
820111	5.45	4.91	4.50	3.45	5.2	2.74	2.20
820331	4.96	4.58	3.90		4.1	2.11	1.40
820402	4.50	3.90			3.7	1.64	
820616	4.85	4.50	3.90		4.0	2.06	1.20
820713	4.25	3.70			3.2	1.44	−0.10
820813	4.66	4.25			3.5	1.88	0.40
831007	5.81	5.30	4.79	3.42	5.0	2.77	2.20
851005	6.18	5.90	5.00		6.7	3.40	3.55
851223	6.18	6.08	5.26		6.8	3.40	3.45
860131	5.54	5.12	4.45	3.02	4.8	2.75	2.10
881125	6.52	6.16	5.68	5.12	5.8	3.61	3.00
891225	5.90	5.45	4.85		5.9	3.30	3.00
901019	5.81	6.10	4.85		4.7	3.06	2.00

relative to that of the earthquake. I also find that the felt area is a better indicator of the high-frequency level than of the 1-Hz level (compare *top* and *bottom* frames of Fig. 3). Finally, felt area is a better predictor of high-frequency level ($\sigma = 0.12$) than is seismic moment ($\sigma = 0.17$, to be shown later). This implies that felt area is more strongly controlled by stress drop than by seismic moment. It supports the contention of Hanks and Johnston (1992) that intensity data may be more diagnostic of real variations in stress drop than are instrumental data (unless the latter are obtained by modern systems capable of recovering high frequencies).

The reason why this is so is that people and objects are most sensitive to the peak of the acceleration spectrum; it controls the ground acceleration and strongly influences the ground velocity. At near-source distances, then, it is obvious that the strength of the felt effects is determined by the amplitude of the high-frequency spectral level. As distance from the earthquake increases, the frequency-band in which the spectral peak is experienced will shift toward lower frequencies, but the peak spectral amplitude remains dependent upon the high-frequency level of the source spectrum. Therefore the strength of the felt effects, even at large distances, measures the high-frequency level of the source spectrum, resulting in an impressive correlation between A_{HF} and a_f. Furthermore, felt area will be more closely related to the high-frequency spectral level than to the 1-Hz spectral level because the 1-Hz amplitude does not necessarily measure the strongest part of the spectrum. Finally, note from equation (1) (assuming $f \gg f_0$) that the high-frequency source level is proportional to $M_0^{0.333} \Delta \sigma^{0.667}$; thus the felt area is more indicative of stress drop than of seismic moment.

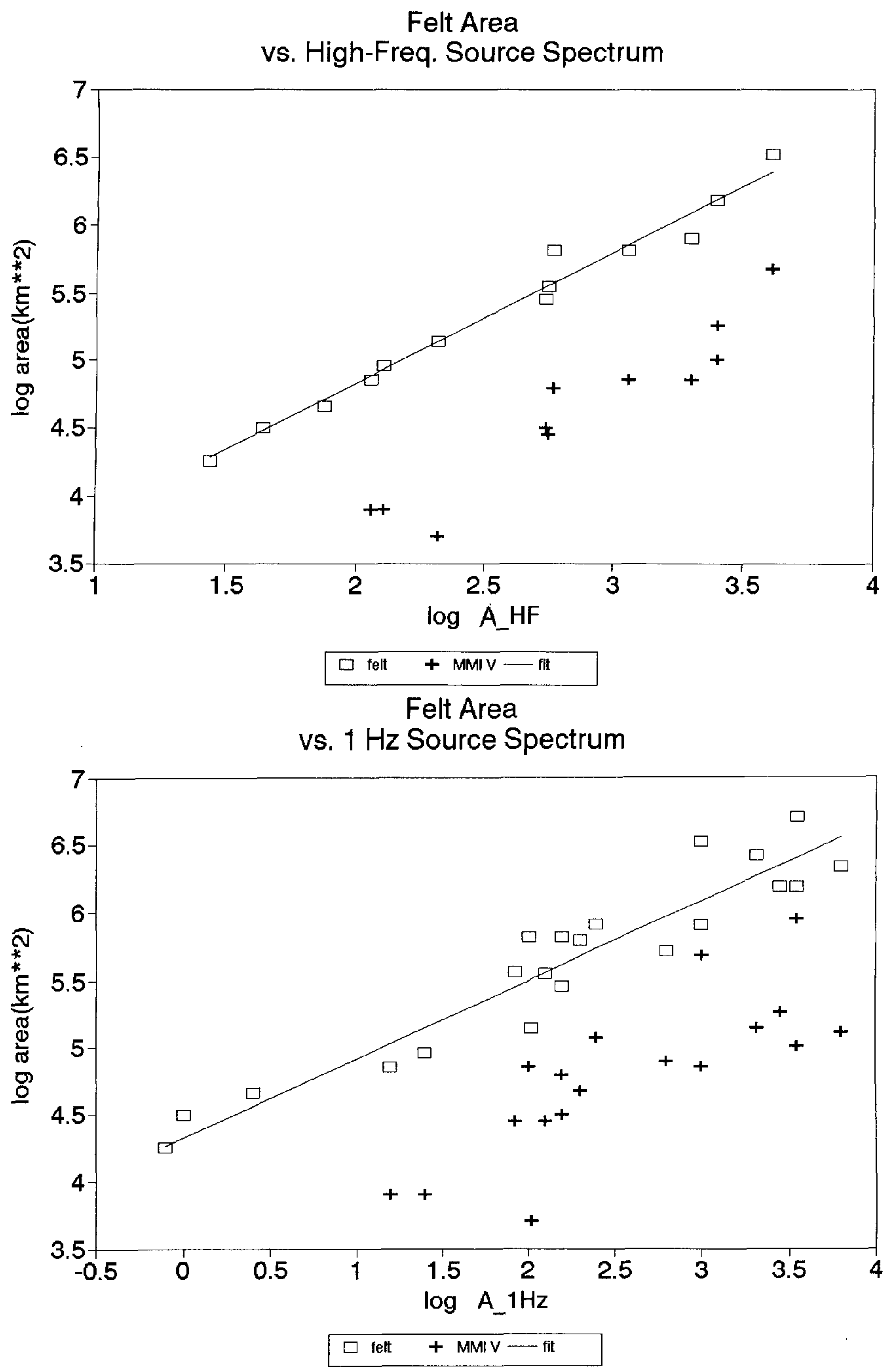

FIG. 3. Felt area (MMI $\geq$ II) as a function of high-frequency source spectral amplitude (*top* frame), and 1 Hz source spectral amplitude (*bottom* frame). Data points for felt area are shown as squares, with lines indicating the least-squares fit. Corresponding areas for MMI V are also shown (plus symbols). All data are from ENA.

ENA Spectral Model

Comparison of Data to Brune Model

Table 1 lists the source parameters for all study events of $\mathbf{M} \geqq 4$. The tabulated spectral amplitudes are for the vertical component; where necessary conversion from horizontal components has been made by subtracting 0.17 log units from the high-frequency spectral level, or 0.05 units from the 1-Hz level (Atkinson, 1993).

Figure 4 plots the observed high-frequency spectral amplitude level for all events as a function of moment magnitude, in comparison to the level predicted by the Brune model (at a frequency of 10 Hz) for stress parameters of 100 and 500 bars (equation 1). For $\mathbf{M} < 4$, the stress parameter seems to increase with $\mathbf{M}$, as is expected due to the finite bandwidth of the ECTN instruments (Boore, 1986). For $\mathbf{M} > 4$, the data are consistent with a constant Brune stress parameter of approximately 200 bars. Different data sources (indicated by different symbols) seem to be mutually consistent, providing further confidence in the robustness of the source-spectral amplitudes. Aftershock data seem to have lower stress parameters than mainshocks, as suggested by Boore and Atkinson (1989). The (unweighted) regression line to the mainshock data, for $\mathbf{M} \geqq 4$ (shown on the figure) is:

$$\log A_{HF} = 0.33 + 0.51\mathbf{M} \tag{4}$$

where A_{HF} is in mm/sec, at a distance of 1 km, for the vertical component. The standard deviation of the residuals (σ) is 0.17 log units. Note that the slope of the line is essentially equal to the value of 0.5 that is required for a constant-stress model.

Figure 5 plots the 1-Hz spectral amplitudes against $\mathbf{M}$. For $\mathbf{M} < 4$ the amplitudes are independent of the stress parameter (we are on the 'moment-end' of the spectrum). For $\mathbf{M} > 4$ the amplitudes are consistent with a constant Brune stress parameter of approximately 50 bars (although 1-Hz amplitudes are not particularly sensitive to the stress parameter until large magnitudes are reached). All plotted data sources, including aftershocks, seem mutually consistent and they have all been included in obtaining the least-squares fit to the 1-Hz spectral amplitude, which for $\mathbf{M} \geqq 4$ is:

$$\log A_{1\ \mathrm{Hz}} = 1.13 + 1.23(\mathbf{M} - 4) - 0.14(\mathbf{M} - 4)^2 \tag{5}$$

with $\sigma = 0.18$. (Note: This regression excluded the outlying point on Figure 5, which is Street and Turcotte's value of $A_{1\ \mathrm{Hz}}$ for the Timiskaming earthquake; this point is suspect because it exceeds the estimated high-frequency level for this event.) The fact that a 50-bar stress parameter matches the 1-Hz spectral amplitude, whereas a 200-bar stress parameter matches the high-frequency level, is further evidence that two corners are required for the spectral model.

Construction of Empirical Source Model

In Figure 6, I construct an empirical two-corner model for ENA source spectra (horizontal component of the shear wave spectrum), for $\mathbf{M} = 4$, 5, 6, and 7, which reconciles all of the available spectral estimates. The primary constraints on the model are the fits to the 1-Hz and high-frequency amplitudes, given by

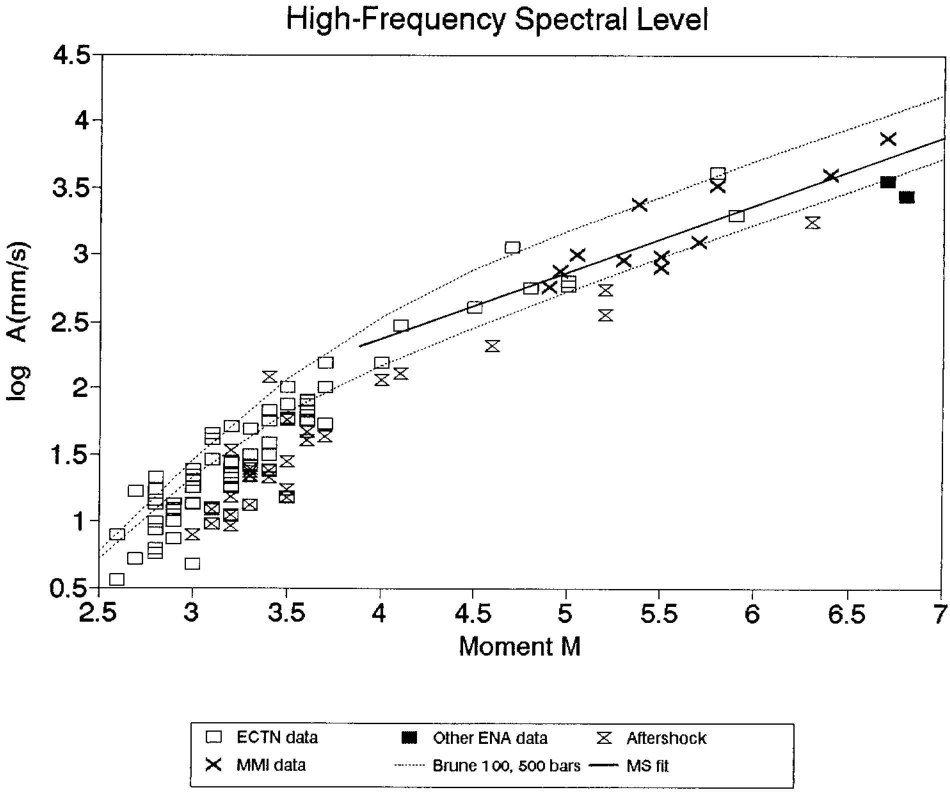

FIG. 4. High-frequency source spectral level (R = 1 km, for vertical component) in ENA, from ECTN data (open squares), MMI data (X's) and strong-motion data (filled squares); all aftershocks are denoted by hourglass symbols. Solid line shows least-squares fit to mainshock data of **M** > 4. Dotted lines show levels for Brune spectrum with stress parameters of 100 bars (lower line) and 500 bars (upper line).

equations 4 and 5 and shown by the plus symbols in Figure 6. The other constraints on the model are that it must converge to the ω^2 source model (equation 1) at low frequencies, at the level determined by the seismic moment. Spectral amplitudes are constant for high frequencies (above the second corner).

A secondary goal, not always compatible with those above, is to match spectral shape data by matching observed corner frequencies. For this purpose I have plotted interpreted lower and upper corner frequencies (Fig. 7). The lower corner frequencies, f_A, are interpreted from the teleseismic data of Boatwright and Choy (1992). They also include the implied corner frequencies from the source duration data of Somerville *et al.* (1987), under the assumption that $f_A = 1/(2T)$, where T is the observed teleseismic duration (Boatwright, personal comm., 1992).

f_A is well constrained by the data. A linear least-squares fit gives:

$$\log f_A = 2.41 - 0.533\mathbf{M}. \tag{6}$$

This equation was used to obtain the f_A values plotted as vertical bars on Figure 6.

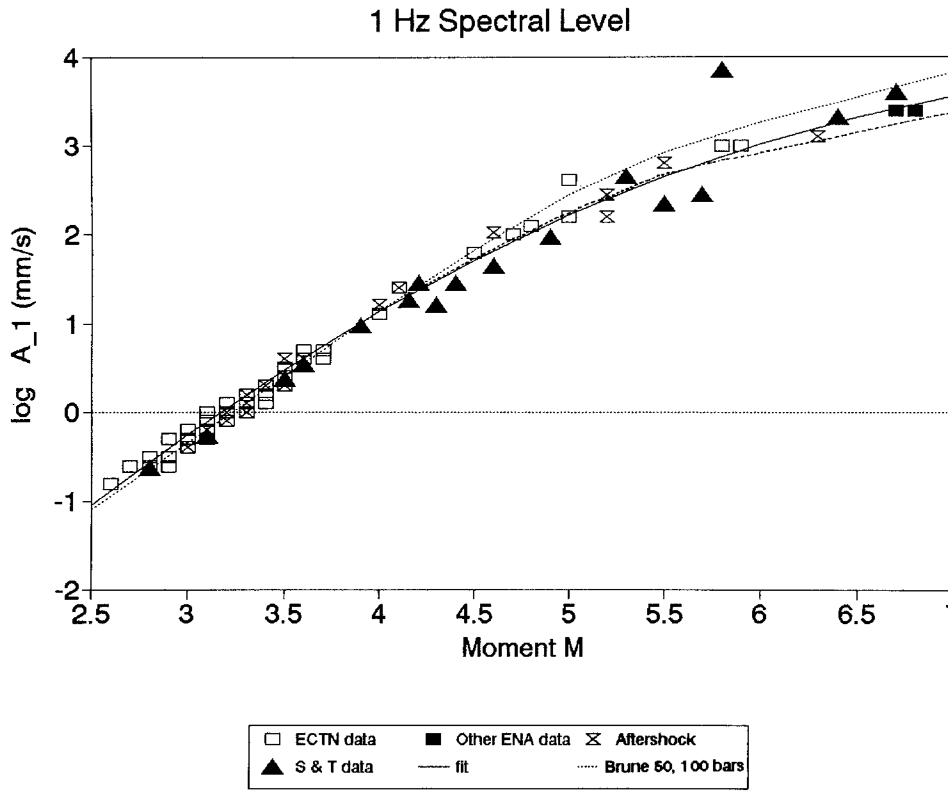

FIG. 5. Source spectral level (R = 1 km, for vertical component) in ENA, at a frequency of 1 Hz, from ECTN data (open squares), historical seismographic data of Street and Turcotte (triangles) and strong-motion data (filled squares); all aftershocks are denoted by hourglass symbols. Solid line shows least-squares fit to all data of **M** > 4. Dotted lines shows levels for Brune spectrum with stress parameters of 50 bars (lower line) and 100 bars (upper line).

The upper corner frequencies, f_B, are based on ECTN data (this study) and strong-motion data (Boore and Atkinson, 1989). They were obtained by finding the frequency at which the spectrum has attained $\frac{1}{2}$ of its full high-frequency level; this definition is used for consistency with the Brune functional form (e.g., in equation (1), $A(f) = A_{HF}/2$ at $f = f_0$).

f_B is not well constrained by data, due to the paucity of high-frequency data for large magnitudes. The fit to these data was therefore used only loosely in constraining the high-frequency shape of the spectrum. Consequently the f_B values implied by the constructed model (plotted on Fig. 7 and given by equation (9)) do not match the data very closely.

The data points on Figure 6 suggest that an appropriate functional form of the empirical model might be derived by adding two Brune spectra (Boore, personal comm., 1992):

$$A(f) = C(2\pi f)^2 M_0\left\{(1-\epsilon)/\left[1+(f/f_A)^2\right] + \epsilon/\left[1+(f/f_B)^2\right]\right\} \tag{7}$$

where ϵ represents some fraction of the total moment. To determine the parameters, I fixed f_A to be given by equation (6). By trial-and-error, I deter-

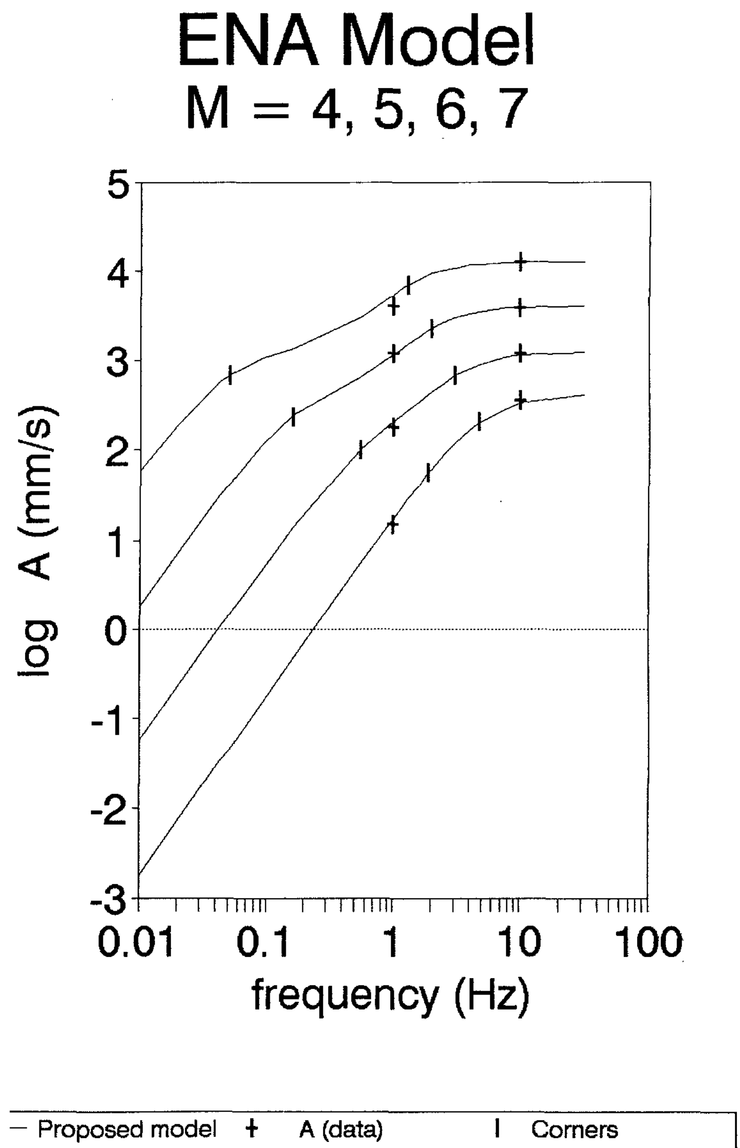

FIG. 6. Proposed two-corner model for ENA source spectral amplitudes (R = 1 km, horizontal component) as a function of frequency, for $\mathbf{M}$ = 4, 5, 6, and 7. Solid lines show the proposed model. Plus symbols show the target levels at 1 Hz and high frequency, obtained from least-squares fit to the data. Vertical bars show the target corner frequencies, f_A and f_B.

mined that all data of $4 \leq \mathbf{M} \leq 7$ can be sensibly fit when:

$$\log \epsilon = 2.52 - 0.637\mathbf{M} \tag{8}$$

$$\log f_B = 1.43 - 0.188\mathbf{M} \tag{9}$$

A measure of how well the model fits the data is provided in Figure 8, which plots the residuals (defined as the difference, in log units, between observations and model predictions) as a function of magnitude, for the 1-Hz and high-

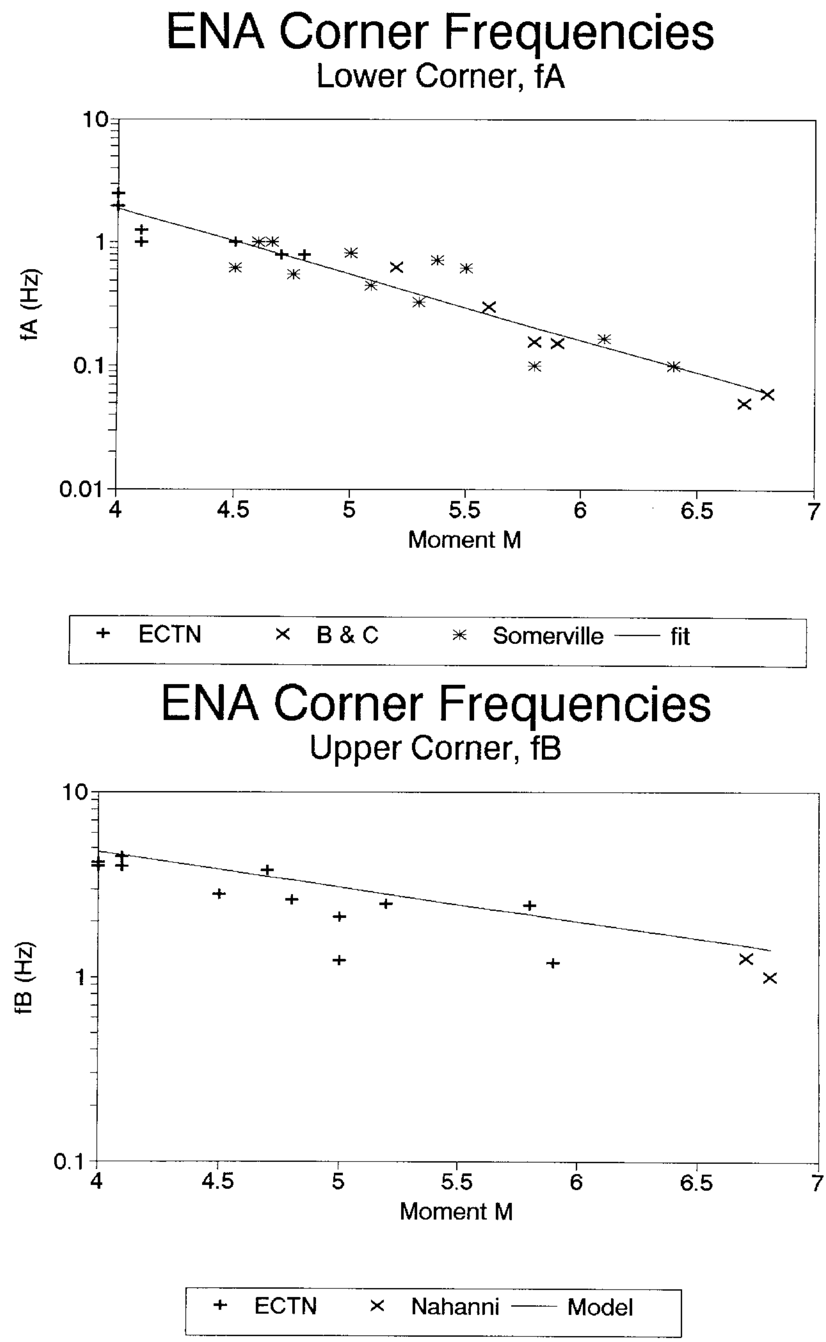

FIG. 7. ENA corner frequency data. The solid line through the f_A data is the least-squares fit to the data. The solid line through the f_B data shows the values required by the empirical model (Equation 9).

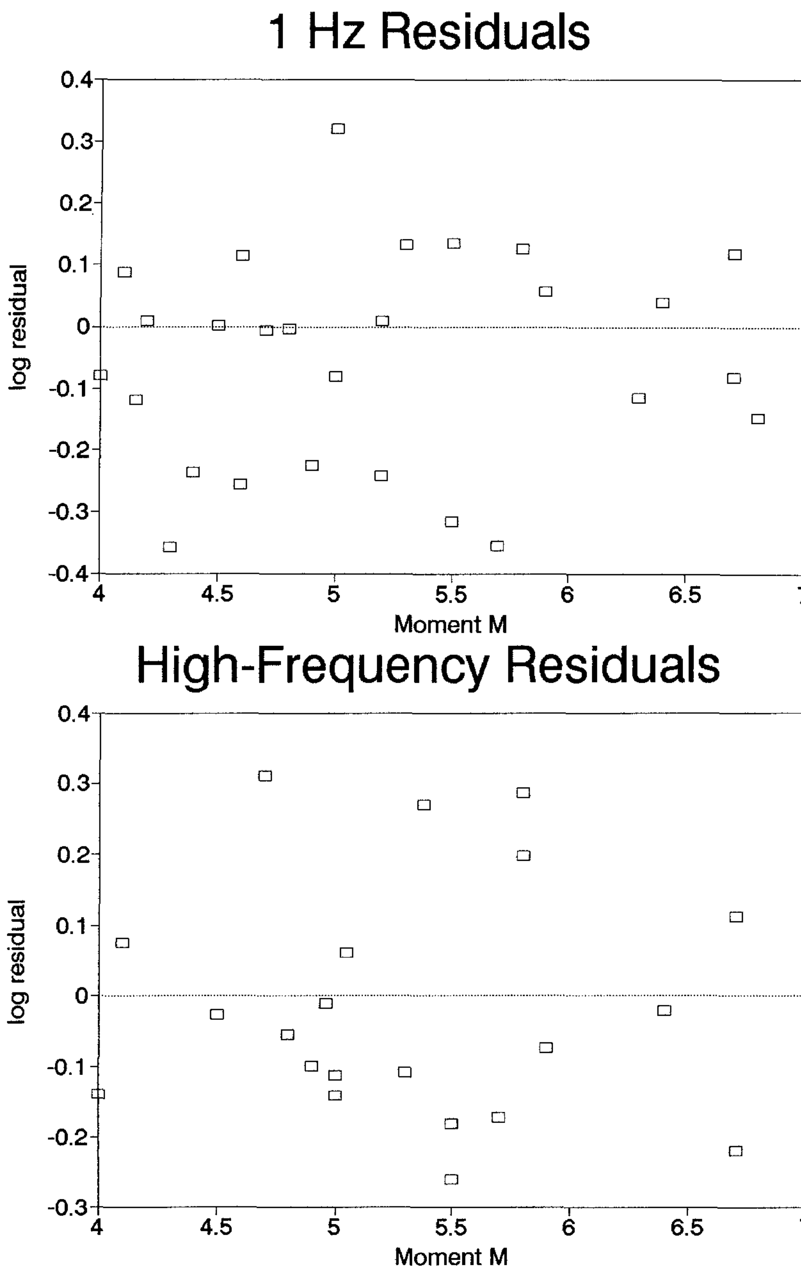

FIG. 8. Residuals for ENA source spectral model as a function of **M**, for a frequency of 1 Hz (*top* frame), and for the high-frequency level (*bottom* frame). (The residual is defined as the ratio of an observed amplitude of the model prediction.) All data used in deriving the model are included.

frequency level. For these data the mean residual is -0.05 at 1 Hz and -0.01 at high frequencies, with standard deviations of 0.17 and 0.16, respectively. In Figure 9, the mean and standard deviation of residuals is plotted as a function of frequency, using just the ECTN data. There are only nine ECTN mainshocks with $\mathbf{M} \geq 4$; two of these events, Saguenay and Mont Laurier, have stress parameters that are much larger than average. As shown in the *top* part of the

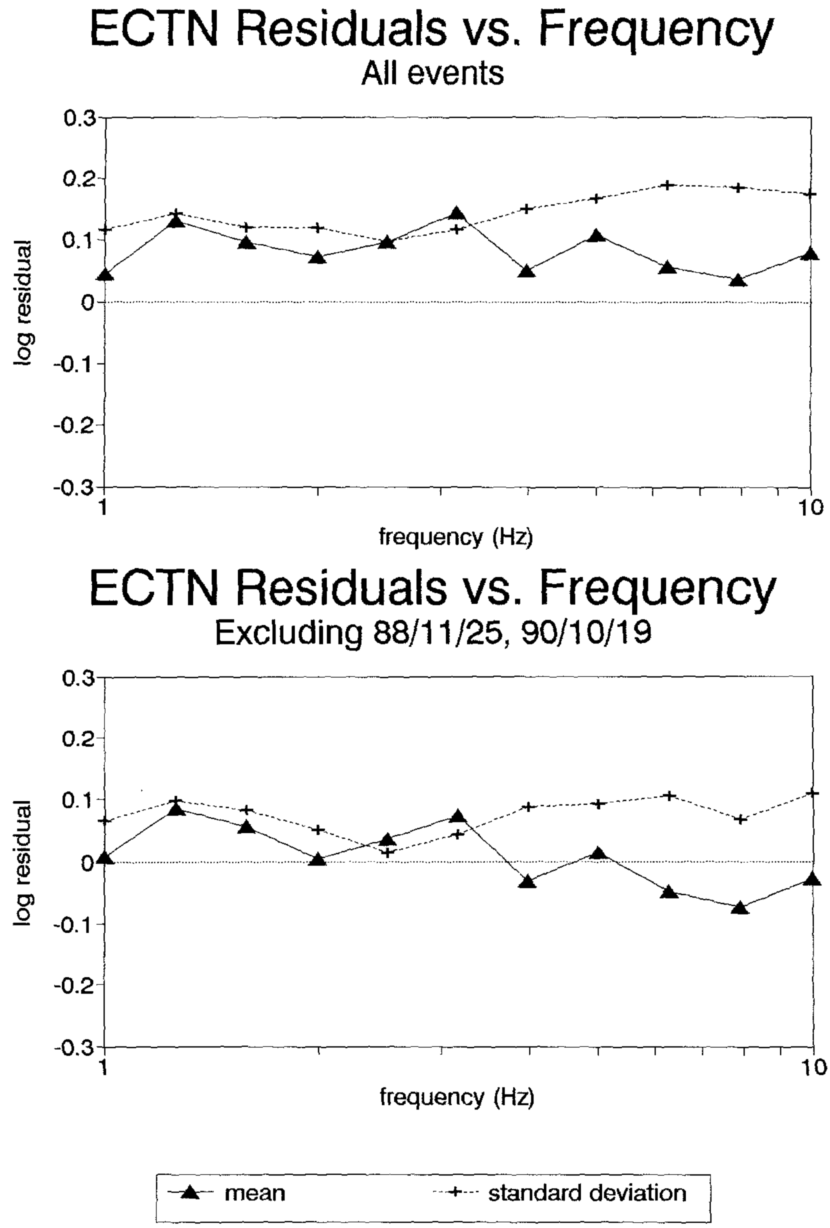

FIG. 9. Mean and standard deviation of residuals for ENA source spectral model, as a function of frequency. *Top* frame includes all ECTN data of **M** > 4 (nine events). *Lower* frame excludes the Saguenay and Mont Laurier earthquakes, which had particularly high stress drops.

figure, their inclusion leads to significant positive residuals. If these two events are omitted (*bottom* part of figure), the residuals are approximately zero. Thus the empirical model accommodates most ENA events, but will underpredict the high-frequency amplitudes from very high-stress events such as Saguenay.

DISCUSSION

I have estimated source spectral amplitudes for ENA earthquakes, and constructed an empirical model that fits these data for events of $4 \leq \mathbf{M} \leq 7$. The functional form (equation 7), involving two corner frequencies, is similar in shape to that proposed for large earthquakes ($\mathbf{M} > 6.5$) by Gusev (1983), on the basis of observed magnitude relationships. In arriving at this shape, Gusev noted that the radiation spectrum of large events may be considered the superposition of radiation from a 'main smooth source' and incoherently combined radiation from a 'subsource population', where a subsource could be any inhomogeneous aspect of the main rupture. Thus the proposed empirical spectra could accommodate, in a general sense, any of the number of possible physical models incorporating some form of 'roughness' (e.g., models featuring partial stress drop, asperities, barriers, etc.). On the other hand, they could also be explained by two characteristic times for the rupture process (i.e., slip rise time and rupture duration), as would be expected for a rectangular fault surface (Haddon, 1992). It is not the intent of equation (7) to supplant or discriminate amongst such possible models.

An interesting observation concerning the high-frequency spectral amplitudes of ENA earthquakes, as shown on Figures 4 and 8, is that there seems to be two classes of events. Most earthquakes of $\mathbf{M} > 4$ have high-frequency spectral amplitudes that are well predicted (i.e., within about 0.15 log units) by a stress parameter of approximately 150 bars. By contrast, four events—the 1988 Saguenay, 1990 Mont Laurier, 1935 Timiskaming, and 1968 Illinois earthquakes—have much larger high-frequency amplitudes; they require, at least in the context of the Brune model, stress parameters of the order of 500 bars. The high stress for the Timiskaming earthquake is speculative because its seismic moment is subject to considerable uncertainty; the strength of the high-frequency amplitudes relative to the low-frequency amplitudes seems to be firmly established for the other three events. The Saguenay and Illinois earthquakes were unusually deep (> 20 km), but the Mont Laurier and Timiskaming earthquakes occurred at 'normal' depths (about 10 km). It may be that ENA crustal conditions, which are characterized by high horizontal compressive stresses and long earthquake repeat times, lead to patches of particularly high stress on the rupture surface in some cases. Alternatively they may lead to unusual rupture geometries, as suggested by Haddon (1992). The possibility of the occurrence of events of this nature implies that the variability of high-frequency ground motions for ENA may be larger than previously recognized. It also implies that Saguenay-type earthquakes, although less common than 150-bar events, are not as anomalous as previously suggested by Boore and Atkinson (1992).

I explored the possibility of using Lg magnitude (M_N), rather than moment magnitude, to predict the high-frequency spectral level, thinking that this might reduce the standard deviation of the high-frequency residuals. One might expect that high-stress events would be characterized by high M_N values. Perhaps surprisingly, I found that M_N does no better than $\mathbf{M}$ as a predictive parameter for the high frequency level; the standard deviation of the spectral amplitude residuals, given $\mathbf{M}_N$, is 0.19, compared with a standard deviation of 0.17, given $\mathbf{M}$. Presumably this is because M_N is generally measured at frequencies lower than the highest corner frequency (except for very large magnitudes, which are sparsely represented in the dataset). I conclude that there is no advantage to using M_N rather than $\mathbf{M}$ in predictive ground motion equations for high-frequency spectral parameters. Because $\mathbf{M}$ is at least tied directly to a particular frequency range of the spectrum, and has a simple physical basis (Hanks and Kanamori, 1979), it remains the best magnitude measure for the spectral

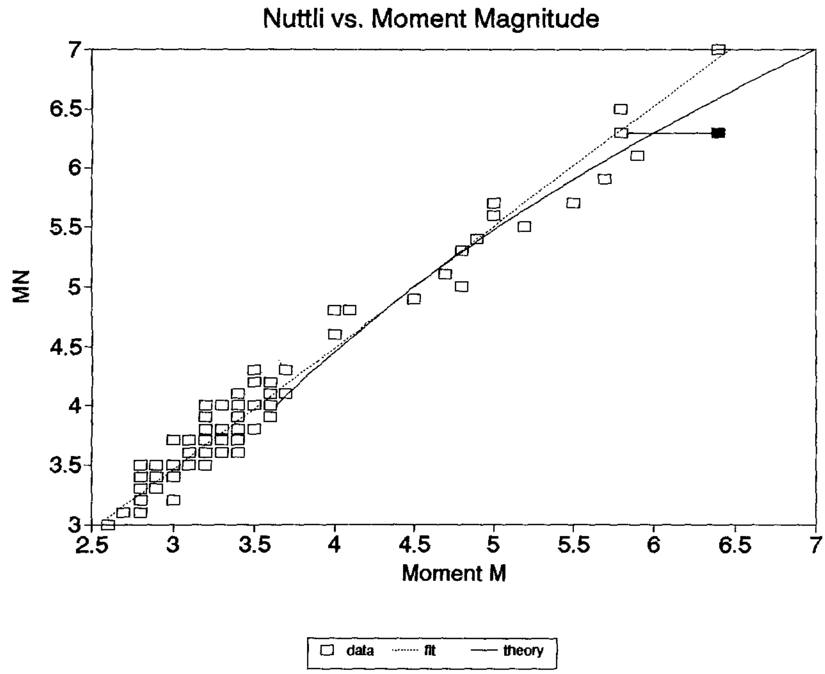

FIG. 10. Relationship between *Lg* magnitude (M_N) and moment magnitude (**M**). Data are from the ECTN (**M** values of this study; M_N values from Geophysics Division, Geological Survey of Canada), and from Boore and Atkinson (1987). Dotted line is the least-squares fit to the data (see Equation 10). Solid line is the theoretical relation of Boore and Atkinson (1987). Filled square shows alternative **M** estimate (Ebel *et al.*, 1986) for the 1935 Timiskaming earthquake.

model. When **M** must be estimated from catalogue values of M_N, the empirical relation obtained from the database may be used:

$$\mathbf{M} = -0.39 + 0.98M_N \qquad M_N < 6 \tag{10}$$

($\sigma = 0.15$). As shown in Figure 10, the empirical data are sufficient to define the relationship well for $3 \leq M_N < 6$. For larger earthquakes, it may be preferable to use a theoretical relationship (e.g., Boore and Atkinson, 1987). The empirical $M_N - \mathbf{M}$ relation is poorly constrained for $M_N > 6$, particularly in light of the large uncertainty in **M** for the 1935 Timiskaming earthquake; I have used the Boore and Atkinson (1987) value of 5.8, whereas Ebel *et al.* (1986) find $\mathbf{M} = 6.4$. (Note: The new moment estimate for the 1925 Charlevoix event by Bent (1992), which corresponds to $\mathbf{M} = 6.3$, is not significantly different from the value of $\mathbf{M} = 6.4$ listed by Boore and Atkinson (1987). The value of $\mathbf{M} = 6.9$ quoted by Ebel *et al.* (1986) was in error (Ebel, personal comm., 1992).)

Figure 11 compares the empirical source model with the 100-bar Brune model, which is the assumption embodied in many ground motion relations (e.g., Boore and Atkinson, 1987; Atkinson and Boore, 1990; Toro and McGuire, 1987; EPRI, 1988). The empirical spectra exceed the Brune 100-bar spectra by a factor of about 1.4 in the 5 to 10 Hz frequency band, for $\mathbf{M} > 5$. For frequencies near 1 Hz, spectral amplitudes are less than those of the 100-bar model, in some cases

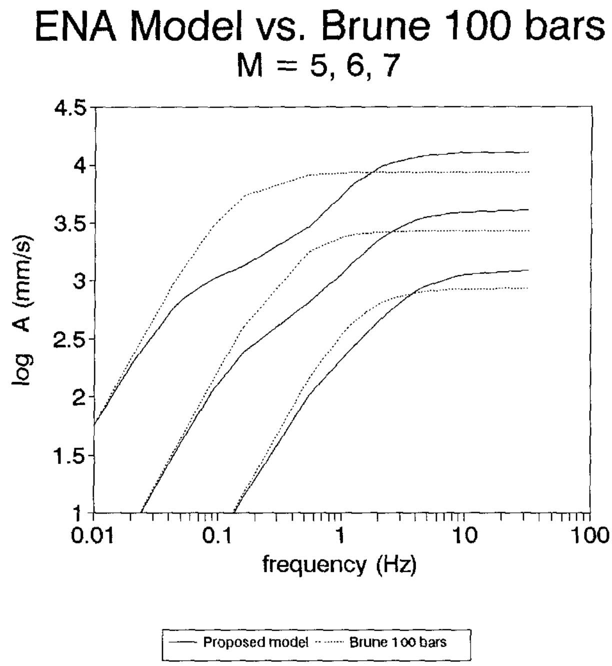

FIG. 11. Comparison of horizontal-component source spectra (R = 1 km) for the ENA empirical model with those of the 100-bar Brune model, for **M** 5, 6, and 7.

by more than a factor of 2. The implied underestimation of the previous ground motion relations at high frequencies is mitigated by the lower crustal constants that were used in those studies ($\rho = 2.7$ gm/cm^3 and $\beta = 3.5$ km/sec); the underestimation of the stress drop was thereby largely offset by overestimation of the scaling constant involving shear wave velocity (equation 1). The net result is that the previous relations are equivalent to using a Brune stress of about 150 bars, with the crustal constants of the current study. Thus the underestimation of the previous ground motion relations at high frequencies is less pronounced than that implied by Figure 11, whereas the overestimation of low frequencies is even more pronounced.

Ground motion relations require significant revision to accommodate the differences between the empirical source model and the 100-bar Brune model. The relative shift in the amplitudes of intermediate-frequency versus high-frequency ground motions has important implications for seismic hazard evaluations and building codes. It suggests that, on a relative scale, the hazard to high-frequency structures in ENA may have been underestimated, whereas hazard to structures of low-to-intermediate frequencies may have been overestimated.

ACKNOWLEDGMENTS

I thank Jack Boatwright, Dave Boore, Tom Hanks, Bob Mereu, and Bill Joyner for many helpful discussions and suggestions. Dave Boore suggested the functional form for the source model. John Anderson provided constructive comments that improved the manuscript. Data were provided by the Geophysics Division of the Geological Survey of Canada; the generous technical support in obtaining and formatting data, provided by Bill Shannon, Bob North, Janet Drysdale, and Wayne McNeil is much appreciated. The financial support of Ontario Hydro is gratefully acknowledged.

REFERENCES

Aki, K. (1982). Strong motion prediction using mathematical modeling techniques. *Bull. Seism. Soc. Am.* **72,** S29–S42.

Atkinson, G. (1984). Attenuation of strong ground motion in Canada from a random vibrations approach. *Bull. Seism. Soc. Am.*, **74,** 26, 29–2653.

Atkinson, G. (1993). H/V ratio for hard-rock sites. *Bull. Seism. Soc. Am.*, **83,** 587–596.

Atkinson, G. and R. Mereu (1992). The shape of ground motion attenuation curves in southeastern Canada. *Bull. Seism. Soc. Am.*, **82,** 2014–2031.

Atkinson, G. and P. Somerville (1993). Calibration of time history simulation methods. *Bull. Seism. Soc. Am.*, submitted.

Bent, A. (1992). A re-examination of the 1925 Charlevoix, Quebec, earthquake. *Bull. Seism. Soc. Am.*, **82,** 2097–2114.

Boatwright, J. (1984). Seismic estimates of stress release. *J. Geophys. Res.*, **89,** B8, 6961–6968.

Boatwright, J. (1988). The seismic radiation from composite models of faulting. *Bull. Seism. Soc. Am.*, **78,** 489–508.

Boatwright, J. (1993). Regional propagation characteristics and source parameters of earthquakes in eastern North America. *Bull. Seism. Soc. Am., in press.*

Boatwright, J. and G. Choy (1992). Acceleration source spectra anticipated for large earthquakes in Northeastern North America. *Bull. Seism. Soc. Am.*, **82,** 660–682.

Boatwright, J., J. Fletcher, and T. Fumal (1991). A general inversion scheme for source, site, and propagation characteristics using multiply recorded sets of moderate-sized earthquakes. *Bull. Seism. Soc. Am.*, **81,** 1783–1812.

Boore, D. (1983). Stochastic simulation of high-frequency ground motions based on seismological models of the radiated spectra. *Bull. Seism. Soc. Am.*, **73,** 1865–1894.

Boore, D. (1986). The effect of finite bandwidth of seismic scaling relationships. *Proc. of the 6th Ewing Symp.*, American Geophysical Union, Geophysical Monograph. **37,** 275–284.

Boore, D. and G. Atkinson (1987). Stochastic prediction of ground motion and spectral response parameters at hard-rock sites in eastern North America. *Bull. Seism. Soc. Am.*, **77,** 440–467.

Boore, D. and G. Atkinson (1989). Spectral scaling of the 1985–1988 Nahanni, Northwest Territories, earthquakes. *Bull. Seism. Soc. Am.*, **79,** 1736–1761.

Boore, D. and G. Atkinson (1992). Source spectra for the 1988 Saguenay, Quebec earthquakes. *Bull. Seism. Soc. Am.*, **82,** 683–719.

Boore, D., W. Joyner, and L. Wennerberg (1992). Fitting the stochastic omega-squared source model to observed response spectra in western North America: trade-offs between stress drop and kappa. *Bull. Seism. Soc. Am.*, **82,** 1956–1963.

Brune, J. (1970). Tectonic stress and the spectra of seismic shear waves from earthquakes. *J. Geophys. Res.*, **75,** 4997–5009.

Burger, R., P. Somerville, J. Barker, R. Herrmann, and D. Helmberger (1987). The effect of crustal structure on strong ground motion attenuation relations in eastern North America. *Bull. Seism. Soc. Am.*, **77,** 420–439.

Choy, G. and J. Boatwright (1988). Teleseismic and near-field analysis of the Nahanni earthquakes, Northwest Territories, Canada. *Bull. Seism. Soc. Am.*, **78,** 1627–1652.

Ebel, J., P. Somerville, and J. McIver (1986). A study of the source parameters of some large earthquakes of northeastern North America. *J. Geophys. Res.*, **91,** B8, 8231–8247.

EPRI, 1988. Engineering model of earthquake ground motion for eastern North America. **EPRI NP-6074,** Electric Power Research Institute, Palo Alto, Calif.

Gusev, A. (1983). Descriptive statistical model of earthquake source radiation and its application to an estimate of short-period strong motion. *Geophys. J. R. Astr. Soc.*, **74,** 787–808.

Haddon, R. (1992). Waveform modeling of the strong-motion data for the Saguenay earthquake of 25 November 1988. *Bull. Seism. Soc. Am.*, **82,** 720–754.

Hanks, T. and A. Johnston (1992). Common features of the excitation and propagation of strong ground motion for North American earthquakes. *Bull. Seism. Soc. Am.*, **82,** 1–23.

Hanks, T. and H. Kanamori (1979). A moment magnitude scale. *J. Geophys. Res.*, **84,** 2348–2350.

Hanks, T. and R. McGuire (1981). The character of high-frequency strong ground motion. *Bull. Seism. Soc. Am.*, **71,** 2071–2095.

Hartzell, S. and J. Brune (1979). The Horse Canyon earthquake of August 2, 1975—Two-stage stress-release process in a strike-slip earthquake. *Bull. Seism. Soc. Am.*, **69,** 1161–1173.

Haskell, N. (1969). Elastic displacements in the near-field of a propagating fault. *Bull. Seism. Soc. Am.*, **59,** 865–908.

Joyner, W. and D. Boore (1982). Prediction of earthquake response spectra. *Proc. of the 51st Annual Conv. Struct. Eng. Assoc.* Calif.

Joyner, W. and D. Boore (1986). On simulating large earthquakes by Green's function addition of smaller earthquakes. In: Earthquake Source Mechanics. Maurice Ewing (Editor), Vol. 6. *American Geophysical Monograph Geophys. Union*, **37,** 269–274.

Kanamori, H. and D. Anderson (1975). Theoretical basis of some empirical relations in seismology. *Bull. Seism. Soc. Am.*, **65,** 1073–1095.

McGarr, A. (1981). Analysis of peak ground motion in terms of a model of inhomogeneous faulting. *J. Geophys. Res.*, **86,** 3901–3912.

Mereu, R., D. Wang, O. Kuhn, D. Forsyth, A. Green, P. Morel, G. Buchbinder, D. Crossley, E. Schwarz, R. duBerger, C. Brooks, and R. Clowes (1986). The 1982 COCRUST seismic experiment across the Ottawa-Bonnechere graben and Grenville Front in Ontario and Quebec. *Geophys. J. R. Astr. Soc.*, **84,** 491–514.

Munro, P., W. Shannon, R. Hallday, and D. Schieman (1986). Canadian seismograph operations—1985. *Seism. Series No. 94,* Earth Physics Branch, Ottawa.

Papageorgiou, A. and K. Aki (1983). A specific barrier model for the quantitative description of inhomoeneous faulting and the prediction of strong ground motion. Part I. Description of the model. *Bull. Seism. Soc. Am.*, **73,** 693–722.

Savage, J. (1972). Relation of corner frequency to fault dimensions. *J. Geophys. Res.*, **77,** 3788–3795.

Sommerville, P., J. McLaren, L. Leevre, R. Burger, and D. Helberger (1987). Comparison of source scaling relations of eastern and western North American earthquakes. *Bull. Seism. Soc. Am.*, **77,** 322–346.

Street, R., and F. Turcotte (1977). A study of northeastern North American spectral moments, magnitudes, and intensities. *Bull. Seism. Soc. Am.*, **67,** 599–614.

Toro, G. and R. McGuire (1987). An investigation into earthquake ground motion characteristics in eastern North America. *Bull. Seism. Soc. Am.*, **77,** 468–489.

Wetmiller, R., R. Horner, H. Hasegawa, R. North, M. Lamontagne, D. Weichert, and S. Evans (1988). An analysis of the 1985 Nahanni earthquakes. *Bull. Seism. Soc. Am.*, **78,** 590–616.

125 Dunbar Rd. S.
Waterloo, Ont. N2L 2E8
Canada

Manuscript received 26 October 1992